# Anisotropic upper critical field and a possible Fulde-Ferrel-Larkin-Ovchinnikov state in a stoichiometric pnictide superconductor LiFeAs

K. Cho,[1] H. Kim,[1,2] M. A. Tanatar,[1] Y. J. Song,[3] Y. S. Kwon,[3]
W. A. Coniglio,[4] C. C. Agosta,[4] A. Gurevich,[5] and R. Prozorov[1,2,*]

[1]*The Ames Laboratory, Ames, IA 50011, USA*
[2]*Department of Physics & Astronomy, Iowa State University, Ames, IA 50011, USA*
[3]*Department of Physics, Sungkyunkwan University, Suwon, Gyeonggi-Do 440-746, Republic of Korea*
[4]*Department of Physics, Clark University, Worcester, MA 01610, USA*
[5]*National High Magnetic Field Laboratory, Florida State University, Tallahhassee, FL 32310, USA*
(Dated: 22 November 2010)

Measurements of the temperature and angular dependencies of the upper critical fields $H_{c2}$ of a stoichiometric single crystal LiFeAs in pulsed magnetic fields up to 50 T were performed using a tunnel diode resonator. Full $H_{c2}^{\|c}(T)$ and $H_{c2}^{\perp c}(T)$ curves with $H_{c2}^{\|c}(0) = 17\pm1$ T, $H_{c2}^{\perp c}(0) = 26\pm1$ T, and the anisotropy parameter $\gamma_H(T) \equiv H_{c2}^{\perp c}/H_{c2}^{\|c}$ decreasing from $\approx 2.5$ at $T_c$ to 1.5 at $T \ll T_c$ were observed. The results for both orientations are in excellent agreement with a theory of $H_{c2}$ for two-band $s^{\pm}$ pairing in the clean limit. We show that $H_{c2}^{\|c}(T)$ is mostly limited by the orbital pairbreaking, whereas the shape of $H_{c2}^{\perp c}(T)$ indicates strong paramagnetic Pauli limiting and the inhomogeneous Fulde-Ferrel-Larkin-Ovchinnikov (FFLO)state below $T_F \sim 5$ K.

There are only few stoichiometric iron-based compounds (Fe-SCs) exhibiting ambient-pressure superconductivity without doping. Among those LiFeAs is unique because of its relatively high $T_c = 18$ K, [1] as compared to LaFePO ($T_c = 5.6$ K) [2] and $KFe_2As_2$ ($T_c = 3$ K) [3]. The absence of doping-induced disorder leads to weak electron scattering, low resistivity, $\rho(T_c) \approx 10\ \mu\Omega$cm [4] and high resistivity ratio, $RRR = \rho(300\text{K})/\rho(T_c) > 30$ [4, 5]. These parameters differ significantly from those of most Fe-SCs for which superconductivity is induced by doping, for example, $Ba(Fe_{1-x}T_x)_2As_2$ [6, 7],$(Ba_{1-x}K_x)Fe_2As_2$ [3] and $BaFe_2(As_{1-x}P_x)_2$ [8]. With the highest $T_c$ among stoichiometric Fe-SCs, negative $dT_c/dP$ [9], tetragonal crystal structure [1, 5] and the absence of antiferromagnetism [10], LiFeAs serves as a model of clean, nearly optimally-doped Fe-SC [4]. Because of very high $H_{c2}$ of Fe-SCs, they may also exhibit exotic behavior caused by strong magnetic fields, for example, the Fulde-Ferrel-Larkin-Ovchinnikov (FFLO) state in which the Zeeman splitting results in oscillations of the order parameter along the field direction [11]. Thus, measurements of $H_{c2}(T)$ in stoichiometric LiFeAs single crystals can reveal manifestations of $s^{\pm}$ pairing in the clean limit [12] for which the FFLO state would be least suppressed by doping-induced disorder [11] as compared to other optimally doped Fe-SCs.

Measurements of the upper critical fields parallel ($H_{c2}^{\|c}$) and perpendicular ($H_{c2}^{\perp c}$) to the crystallographic $c-$axis in many Fe-Sc have shown several common trends [6, 7, 13–27]. Close to $T_c$ where $H_{c2}$ is limited by orbital pairbreaking, the anisotropy parameter $\gamma_H \equiv H_{c2}^{\perp c}/H_{c2}^{\|c}$ ranges between 1.5 and 5 [13, 18, 23–26], in agreement with the anisotropy of the normal state resistivity $\gamma_H = (\rho_c/\rho_{ab})^{1/2}$ above $T_c$ [7]. As $T$ decreases, $H_{c2}(T)$ becomes more isotropic [18, 20, 27], consistent with multiband pairing scenarios and the behavior of $H_{c2}$ in dirty $MgB_2$ [28], yet opposite to clean $s^{++}$ $MgB_2$ single crystals [29]. However, the more isotropic $H_{c2}$ at low $T$ can also result from strong Pauli pairbreaking for $\mathbf{H}\|ab$ since the observed $H_{c2}$ on many Fe-SCs significantly exceeds the BCS paramagnetic limit $H_p(T) = 1.84T_c(K)$ [17, 18, 25–27, 30]. Thus, measuring $H_{c2}$ in LiFeAs can probe the interplay of orbital and Pauli pairbreaking in the clean $s^{\pm}$ pairing limit at high magnetic fields. These measurements are also interesting because magnetic fluctuations may contain significant ferromagnetic contribution which may lead to triplet pairing [31]. Experimentally, vortex properties of LiFeAs were found to be very similar to the supposedly triplet $Sr_2RuO_4$ [32], although NMR studies suggest singlet pairing [33]. Triplet superconductors can exhibit unusual response to magnetic field [34], and, indeed, candidate materials show pronounced anomalies, as observed in $UPt_3$ [35, 36] and $Sr_2RuO_4$ [37]. Surprisingly, our measurements show that normalized $H_{c2}^{\perp c}$ of LiFeAs matches quite closely that of $Sr_2RuO_4$.

We present the measurements of the complete $H-T$ phase diagram of LiFeAs in pulsed magnetic fields up to 50 T, and down to 0.6 K using a tunnel diode resonator (TDR) technique. We found that $H_{c2}^{\perp c}(T)$ shows rapid saturation at low temperatures, consistent with strong Pauli pairbreaking. Our data can be described well by a theory of $H_{c2}$ for the multiband $s^{\pm}$ pairing in the clean limit [38], which also suggests the FFLO state in LiFeAs for $H\perp c$ below 5 K. Previous measurements of $H_{c2}$ in LiFeAs were performed at relatively low fields [5, 39], thus not allowing to reveal the spin-limited behavior at low $T$. The only high-field torque measurements of

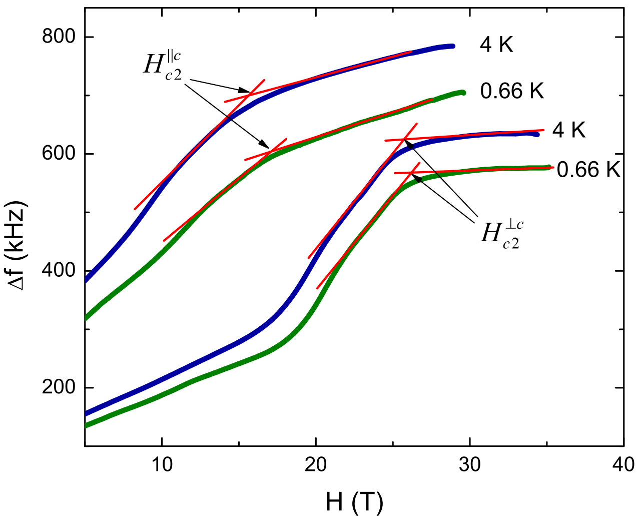


FIG. 1. (Color online) TDR frequency change for increasing pulsed magnetic field, appied in two orientations, $H \parallel c$ and $H \perp c$, shown for two temperatures for sample A. The definition of $H_{c2}$ is shown as the intersection of two straight lines below and above the transition.

the irreversibility field, $H_{irr}(T)$ were recently reported in Ref. [40]. However, $H_{irr}(T)$ may not only underestimate the true $H_{c2}(T)$ but also have a different temperature dependence due to the effects of pinned vortex liquid at $H \approx H_{irr}$, as well as sample shape anisotropy, as observed in high$-T_c$ cuprates [41].

Single crystals of LiFeAs were grown in a sealed tungsten crucible using Bridgeman method and placed in ampoules. Immediately after opening, samples were covered with Apiezon N grease, which provides some degree of short-term protection [4]. The samples were cleaved and cut inside the grease layer to minimize exposure to the air. The two studied samples had dimensions of $0.6 \times 0.5 \times 0.1$ mm$^3$ (sample A) and $0.9 \times 0.8 \times 0.2$ mm$^3$ (sample B). Superconducting transition temperature for both samples was $T_c = 17.6 \pm 0.1$ K (more than 10% higher than $T_c = 15.5$ K of Ref. 40). Dynamic magnetic susceptibility $\chi$ was measured with 190 MHz (sample A) and 16 MHz (sample B) TDR [42]. The magnetic field was generated by a 50 T pulsed magnet with a 11 ms rise time at Clark University. A single-axis rotator with a $0.5^\circ$ angular resolution was used to accurately align the sample with respect to the $c-$axis (see inset in Fig. 2(a)). The data have been taken for each orientation at temperatures down to 0.66 K. The normal state data at 25 K have also been taken for both orientations and subtracted. Measured shift of the resonant frequency $\Delta f \propto \chi$ [42], thus exhibits a kink at $H_{c2}$ where London penetration depth diverges and is replaced by the normal - state skin depth. Thus, barring uncertainty due to fluctuations, it is probing a "true" upper critical field.

Fig. 1 shows the change of the resonant frequency as a function of $H$ for sample A for two field orientations and two temperatures. From many such traces, both $H_{c2}^{\perp c}$ and $H_{c2}^{\|c}$ were determined as shown in Fig. 1 and are plotted in Fig. 2. Figure 2(a) compares our data on samples A and B with the previous transport measurements of $H_{c2}$ [5, 39, 43] and $H_{irr}$ from torque measurements [40]. Figure 2(a) also shows the behavior expected from the orbital Werthamer-Helfand-Hohenberg (WHH) theory [44] with $H_{\rm orb}(0) = 0.69T_{\rm c}|dH_{\rm c2}/dT|_{\rm T_c}$, the single-gap BCS paramagnetic limit, $H_P^{BCS} = 1.84T_c = 32.2$ T, as well as $H_P^{\Delta_1} = 34.7$ T and $H_P^{\Delta_2} = 20.4$ T calculated with $\Delta_1(0)/{\rm T}_c \approx 1.885$ and $\Delta_1(0)/{\rm T}_c \approx 1.111$ reported for the same samples in Ref. [4]. Clearly, the observed $H_{c2}(T)$ exhibits much stronger flattening at low temperature compared to the orbital WHH theory. Inset in Fig. 2(a) shows the dependence of $H_{c2}$ on the angle between $\mathbf{H}$ and the $ab$ plane at 0.66 K where $H_{c2}^{\perp c}$ is defined at a maximum of $H_{c2}(\varphi) = H_{c2}^{\|c} + (H_{c2}^{\perp c} - H_{c2}^{\|c})\cos\varphi$ depicted by the solid line.

We analyze our $H_{c2}(T)$ data using a two-band theory, which takes into account both orbital and paramagnetic pairbreaking in the clean limit, and the possibility of the FFLO with the wave vector $Q(T,H)$. In this case the equation for $H_{c2}$ is given by [38],

$$a_1 G_1 + a_2 G_2 + G_1 G_2 = 0, \tag{1}$$

$$G_1 = \ln t + 2e^{q^2}\,\mathrm{Re}\sum_{n=0}^{\infty}\int_q^{\infty} du e^{-u^2} \times \left[\frac{u}{n+1/2} - \frac{t}{\sqrt{b}}\tan^{-1}\left(\frac{u\sqrt{b}}{t(n+1/2)+i\alpha b}\right)\right]. \tag{2}$$

Here $Q(T,H)$ is determined by the condition that $H_{c2}(T,Q)$ is maximum, $a_1 = (\lambda_0 + \lambda_-)/2w$, $a_2 = (\lambda_0 - \lambda_-)/2w$, $\lambda_- = \lambda_{11} - \lambda_{22}$, $\lambda_0 = (\lambda_-^2 + 4\lambda_{12}\lambda_{21})^{1/2}$, $w = \lambda_{11}\lambda_{22} - \lambda_{12}\lambda_{21}$, $t = T/T_c$, and $G_2$ is obtained by replacing $\sqrt{b} \to \sqrt{\eta b}$ and $q \to q\sqrt{s}$ in $G_1$, where

$$b = \frac{\hbar^2 v_1^2 H}{8\pi\phi_0 k_B^2 T_c^2 g_1^2}, \qquad \alpha = \frac{4\mu\phi_0 g_1 k_B T_c}{\hbar^2 v_1^2}, \tag{3}$$

$$q^2 = Q_z^2 \phi_0 \epsilon_1 / 2\pi H, \qquad \eta = v_2^2/v_1^2, \qquad s = \epsilon_2/\epsilon_1. \tag{4}$$

Here $v_l$ is the in-plane Fermi velocity in band $l = 1, 2$, $\epsilon_l = m_l^{ab}/m_l^c$ is the mass anisotropy ratio, $\phi_0$ is the flux quantum, $\mu$ is the magnetic moment of a quasiparticle, $\lambda_{11}$ and $\lambda_{22}$ are the intraband pairing constants, and $\lambda_{12}$ and $\lambda_{21}$ are the interband pairing constants, and $\alpha \approx 0.56\alpha_M$ where the Maki parameter $\alpha_M = H_{c2}^{orb}/\sqrt{2}H_p$ quantifies the strength of the Zeeman pairbreaking. The factors $g_1 = 1 + \lambda_{11} + |\lambda_{12}$ and $g_2 = 1 + \lambda_{22} + |\lambda_{21}|$ describe the strong coupling Eliashberg corrections. For the sake of simplicity, we consider here the case of $\epsilon_1 = \epsilon_2 = \epsilon$ for which $H_{c2}^{\perp c}$ is defined by Eqs. (1) and (2) with $g_1 = g_2$ and rescaled $q \to q\epsilon^{-3/4}$, $\alpha \to \alpha\epsilon^{-1/2}$ and $\sqrt{b} \to \epsilon^{1/4}\sqrt{b}$ in $G_1$ and $\sqrt{\eta b} \to \epsilon^{1/4}\sqrt{\eta b}$ in $G_2$ [38].

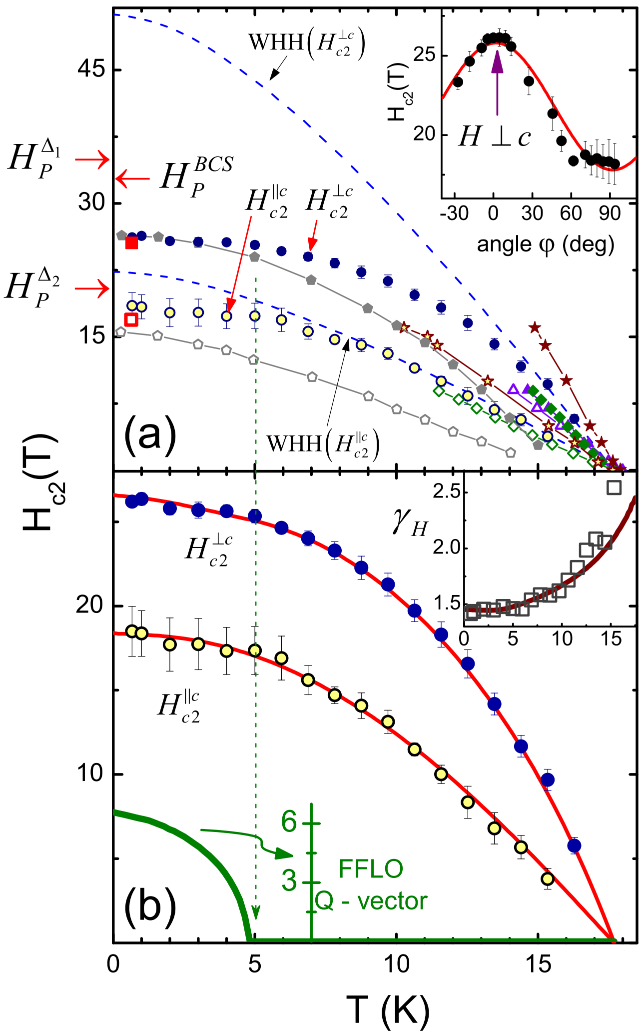


FIG. 2. (Color online) (a) $H_{c2}(T)$ for $H\perp c$ (solid symbols) and $H \parallel c$ (open symbols). Blue circles and red squares correspond to samples A and B, respectively. For comparison we show the literature data determined from the resistivity measurements with mid-point criterion: (magenta) triangles [5], (green) rhombi [39] and (brown) stars [43]. Grey pentagons are torque $H_{irr}$ [40]. Dashed lines is the WHH $H_{c2}(T)$. Inset in (a) shows $H_{c2}(\varphi)$ at 0.66 K where the solid line is $H_{c2}(\varphi) = H_{c2}^{\parallel c} + (H_{c2}^{\perp c} - H_{c2}^{\parallel c})\cos\varphi$. (b) Fit of the experimental data to $H_{c2}(T)$, $Q(T)$ and $\gamma_H(T)$ (solid lines) calculated from Eq. (1) for the parameters given in the text. The FFLO wave vector $Q(T)$ is plotted in the units of $40\pi k_B T_c g_1/\hbar v_1$, and the inset shows the anisotropy parameter $\gamma_H(T)$.

Figure 2(b) shows the fit of the measured $H_{c2}(T)$ to Eq. (1) for $s^{\pm}$ pairing with $\lambda_{11} = \lambda_{22} = 0$, $\lambda_{12}\lambda_{21} = 0.25$, $\eta = 0.3$, $\alpha = 0.35$, and $\epsilon = 0.128$. Equation (1) describes $H_{c2}^{\parallel c}$(T), $H_{c2}^{\perp c}$(T) and $\gamma_H(T) = b_{\parallel}(T)/\sqrt{\epsilon}\, b_{\perp}(T)$ where $b_{\parallel}(T)$ and $b_{\perp}(T)$ are the solutions of Eq. (1) for $H\|c$ and $H\perp c$, very well. The fit parameters are also in good quantitative agreement with experiment. For instance, the Fermi velocity $v_1 = (g_1 k_B T_c/\hbar)[8\pi\phi_0 b_{\perp}(0)/H_{c2}^{\parallel c}(0)]^{1/2}$ can be expressed from Eq. (4) in terms of materials parameters and $b_{\perp}(0) = 0.314$ calculated from Eq. (1). For $T_c = 17.8$ K, $H_{c2}^{\parallel c}(0) = 18.4$T and $g = 1.5$ for $\lambda_{12} = 0.5$, we obtain $v_1 = 1.12\times 10^7$ cm/s, consistent with the ARPES results [10].

Several important conclusions follow from the results shown in Fig. 2(b). First, contrary to the single-band Ginzburg-Landau scaling, $\gamma_H^{GL} = \epsilon^{-1/2}$, the anisotropy parameter $\gamma_H(T)$ decreases as $T$ decreases. Not only is this behavior indicative of multiband pairing [28], but it also reflects the significant role of the Zeeman pairbreaking in LiFeAs given that $\alpha_{\|} = \alpha/\sqrt{\epsilon} = 0.98$ for $H\perp c$ is close to the single-band FFLO instability threshold, $\alpha \approx 1$ [38]. In this case $\gamma_H(T)$ near $T_c$ is determined by the orbital pairbreaking and the mass anisotropy $\epsilon$, but as $T$ decreases, the contribution of the isotropic paramagnetic pairbreaking increases, resulting in the decrease of $\gamma_H(T)$. Another intriguing result is that the solution of Eq. (1) shows no FFLO instability for $H\|c$, but predicts the FFLO transition at $T < T_F \approx 5$ K for $H\|ab$. The FFLO wave vector $Q(T) = 4\pi k_B T_c q(T) b^{1/2}(T) g_1/\hbar v_1$ appears spontaneously at $T = T_F \approx 5$ K where the FFLO period $\ell = 2\pi/Q = \hbar v_1/2k_B T_c g_1 q(T) b^{1/2}(T)$ diverges and then decreases as $T$ decreases, reaching $\ell(0) = \pi\xi_0/g_1 q(0) b^{1/2}(0) \approx 9\xi_0$ at $T = 0$. Here $q(0) = 0.656$, $b(0) = 0.126$, and $\xi_0 = \hbar v_1/2\pi k_B T_c \simeq 7.3$ nm, giving $\ell(0) \simeq 65.6$ nm for the parameters used above. The period $\ell(0)$ is much smaller than the mean free path, $\ell_{mfp} \sim 550$ nm, estimated from the Drude formula for an ellipsoidal Fermi surface with $\epsilon = 0.128$, $v_F = 112$ km/s, $m_{ab}$ equal to the free electron mass, and $\rho(T_c) = 10\mu\Omega$cm. Notice that $\rho(T_c)$ may contain a significant contribution from inelastic scattering, so the mean free path for elastic impurity scattering which destroys the FFLO state [11] is even larger than $\ell_{mfp}$. Therefore, the FFLO state found in our calculations may be a realistic possibility verifiable by specific heat, magnetic torque and thermal conductivity measurements.

Finally, we compare LiFeAs with other superconductors, especially those for which $H_{c2}$ is clearly limited by either orbital or Zeeman pairbreaking mechanisms. Shown in Fig. 3 are the plots of the normalized $H_{c2}(T)/T_c H'_{c2}$ as functions of $T/T_c$ for the $\mathbf{H}\|ab$ orientation where the Zeeman pairbreaking is most pronounced. Here $H'_{c2} = |dH_{c2}/dT|_{T\to T_c}$ and our data are shown by the thick solid black line, whereas the literature data are shown by symbols. The reference materials include: $H_{irr}$ for LiFeAs [40]; $H_{c2}$ for the Pauli-limited [45] organic superconductor $\kappa$-(BEDT-TTF)$_2$Cu[N(CN)$_2$]Br [46]; heavy fermion $CeCoIn_5$ [47]; optimally-doped iron pnictides, Ba(Fe$_{1-x}$Co$_x$)$_2$As$_2$ [18] and Ba$_x$K$_{1-x}$FeAs$_2$ [20] as well as iron chalcogenide Fe(Se,Te) [27]. Conventional NbTi is also shown by open pentagons [48]. From this comparison, it appears that LiFeAs is indeed closer to the paramagnetic limit. Notably, the data for LiFeAs lay below other iron-based superconductors, except for the highest purity ($RRR \sim 1000$) $KFe_2As_2$ [49]. On the

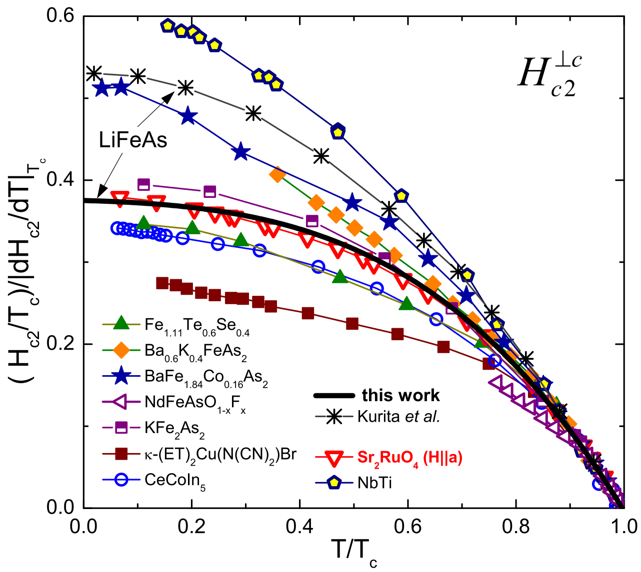


FIG. 3. (Color online) $(H_{c2}(T)/T_c)/|dH_{c2}/dT|_{T_c}$ vs. $T/T_c$ in the $H\perp c$ orientation. Black solid line is our data in comparison with several Fe-SCs as well as other exotic superconductors and conventional NbTi, all shown in the legend.

other hand, our data appear above $CeCoIn_5$, believed to be mostly Pauli limited [47]. Interestingly, the data for LiFeAs stay almost on top of the $H_{c2}(T)$ for $Sr_2RuO_4$, in which limiting of $H_{c2}$ proceeds in a very unusual manner, leading to the formation of the second superconducting phase [37]. Given that vortex dynamics in these two materials is also similar [32], the coincidence of the $H_{c2}(T)/T_c H'_{c2}$ curves is worth of further exploration.

Summarizing, full - temperature range experimental $H_{c2}^{\parallel c}(T)$ and $H_{c2}^{\perp c}(T)$ deviate significantly from the single-band WHH behavior but are in excellent agreement with the theory of $H_{c2}$ for the $s^{\pm}$ pairing in the clean limit. Our results indicate Pauli-limited behavior and the FFLO state below 5 K for $H\perp c$.

We thank A. Carrington, V. G. Kogan and L. Taillefer for discussions. The work at Ames was supported by DOE BES under contract No. DE-AC02-07CH11358. The work at Clark was supported by DOE under contract No. ER46214. The work at Sungkyunkwan University was supported by the Basic Science Research Program (2010-0007487), the Mid-career Researcher Program (No.R01-2008-000-20586-0). R. P. acknowledges support from Alfred P. Sloan Foundation. A. G. was supported by NSF through NSF-DMR-0084173 and by the State of Florida.

* Corresponding author: prozorov@ameslab.gov


[1] X. C. Wang *et al.*, Solid State Comm. **148**, 538 (2008).
[2] Y. Kamihara *et al.*, J. Am. Chem. Soc. **128**, 10012 (2006).
[3] M. Rotter *et al.*, Phys. Rev. Lett. **101**, 107006 (2008).
[4] H. Kim *et al.*, arXiv:1008.3251 (2010).
[5] Y. J. Song *et al.*, Appl. Phys. Lett. **96**, 212508 (2010).
[6] N. Ni *et al.*, Phys. Rev. B **82**, 024519 (2010).
[7] M. A. Tanatar *et al.*, Phys. Rev. B **79**, 094507 (2009).
[8] S. Kasahara *et al.*, Phys. Rev. B **81**, 184519 (2010).
[9] C. W. Chu *et al.*, Physica C **469**, 326 (2009).
[10] S. V. Borisenko *et al.*, Phys. Rev. Lett.**105**, 067002 (2010).
[11] Y. Matsuda and H. Shimahara, J. Phys. Soc. Jpn. **76**, 051005 (2007).
[12] I. Mazin *et al.*, Phys. Rev. Lett.**101**, 057003 (2008); K. Kuroki *et al.*, Phys. Rev. Lett.**101**, 087004 (2008); V. Mishra *et al.*, Phys. Rev. B**79**, 094512 (2009).
[13] F. Hunte *et al.*, Nature **453**, 903 (2008).
[14] Y. Jia *et al.*, App. Phys. Lett. **93**, 032503 (2008).
[15] J. Kacmarcik *et al.*, Phys. Rev. B **80**, 014515 (2009).
[16] H. Lee *et al.*, Phys. Rev. B **80**, 144512 (2009).
[17] J. Jaroszynski *et al.*, Phys. Rev. B **78**, 174523 (2008).
[18] M. Kano *et al.*, J. Phys. Soc. Japan **78**, 084719 (2009).
[19] Z. Bukowski *et al.*, Phys. Rev. B **79**, 104521 (2009).
[20] H. Q. Yuan *et al.*, Nature **457**, 565 (2009).
[21] S. Jiang *et al.*, Phys. Rev. B **80**, 184514 (2009).
[22] N. P. Butch *et al.*, Phys. Rev. B **81**, 024518 (2010).
[23] D. Braithwaite *et al.*, J. Phys. Soc. Jpn. **79**, 053703 (2010).
[24] H. Lei *et al.*, Phys. Rev. B **81**, 184522 (2010).
[25] T. Kida *et al.*, J. Phys. Soc. Jpn. **79**, 074706 (2010).
[26] S. Khim *et al.*, Phys. Rev. B **81**, 184511 (2010).
[27] M. Fang *et al.*, Phys. Rev. B **81**, 020509(R) (2010).
[28] A. Gurevich, Phys. Rev. B **67**, 184515 (2003).
[29] V. G. Kogan and S. L. Bud'ko, Physica C **385**, 131 (2003).
[30] G. Fuchs *et al.*, Phys. Rev. Lett.**101**, 237003 (2008) and New J. Phys. **11**, 075007 (2009); A. Yamamoto *et al.*, Appl. Phys. Lett. **94**, 062511 (2009); M. Altarawneh *et al.*, Phys. Rev. B**78**, 220505 (R) (2008).
[31] T. M. Rice and M. Sigrist, J. Phys.:Cond. Matt. **7**, L643 (1995).
[32] A. K. Pramanik *et al.*, arXiv:1009.4896 (2010).
[33] Z. Li *et al.*, J. Phys. Soc. Japan **79**, 083702 (2010).
[34] A. G. Lebed and N. Hayashi, Physica C **341**, 1677 (2000).
[35] H. Suderow *et al.*, Phys. Rev. Lett. **80**, 165 (1998).
[36] K. Hasselbach *et al.*, Phys. Rev. Lett. **63**, 93 (1989).
[37] K. Deguchi *et al.*, J. Phys. Soc. Japan **71**, 2839 (2002).
[38] A. Gurevich, Phys. Rev. B **82**, 184504 (2010).
[39] B. Lee *et al.*, Europhys. Lett. **91**, 67002 (2010).
[40] N. Kurita *et al.*, arXiv:1011.1334 (2010).
[41] A. Carrington *et al.*, Phys. Rev. B **54** 3788 (1996).
[42] R. Prozorov and R. W. Giannetta, Supercond. Sci. Technol. **19**, R41 (2006).
[43] O. Heyer *et al.*, arXiv:1010.2876 (2010).
[44] N. R. Werthamer *et al.*, Phys. Rev. **147**, 295 (1966).
[45] A. E. Kovalev *et al.*, Phys. Rev. B **62**, 103 (2000).
[46] E. Ohmichi *et al.*, Syn. Metals **133**, 245 (2003).
[47] A. Bianchi *et al.*, Phys. Rev. Lett. **91**, 187004 (2003).
[48] Y. Shapira and L. J. Neuringer, Phys. Rev. **140**, A1638 (1965).
[49] T. Terashima *et al.*, J. Phys. Soc. Japan **78**, 063702 (2009).